

REPORT

 OPEN ACCESS

## Generation, characterization and preclinical studies of a human anti-L1CAM monoclonal antibody that cross-reacts with rodent L1CAM

Seulki Cho<sup>a,b</sup>, Insoo Park<sup>c,\*</sup>, Haejung Kim<sup>b</sup>, Mun Sik Jeong<sup>d</sup>, Mooney Lim<sup>d</sup>, Eung Suk Lee<sup>b,\*\*</sup>, Jin Hong Kim<sup>b</sup>, Semi Kim<sup>c</sup>, and Hyo Jeong Hong<sup>b,d</sup>

<sup>a</sup>Department of Functional Genomics, University of Science & Technology, Daejeon, Korea; <sup>b</sup>Institute of Bioscience and Biotechnology, Kangwon National University, Chuncheon, Korea; <sup>c</sup>Immunotherapy Research Center, Korea Research Institute of Bioscience & Biotechnology, Daejeon, Korea; <sup>d</sup>Department of Systems Immunology, Kangwon National University, Chuncheon, Korea

### ABSTRACT

L1 cell adhesion molecule (L1CAM) is aberrantly expressed in malignant tumors and plays important roles in tumor progression. Thus, L1CAM could serve as a therapeutic target and anti-L1CAM antibodies may have potential as anticancer agents. However, L1CAM is expressed in neural cells and the druggability of anti-L1CAM antibody must be validated at the earliest stages of preclinical study. Here, we generated a human monoclonal antibody that is cross-reactive with mouse L1CAM and evaluated its pharmacokinetic properties and anti-tumor efficacy in rodent models. First, we selected an antibody (Ab4) that binds human and mouse L1CAM from the human naïve Fab library using phage display, then increased its affinity 45-fold through mutation of 3 residues in the complementarity-determining regions (CDRs) to generate Ab4M. Next, the affinity of Ab4M was increased 1.8-fold by yeast display of single-chain variable fragment containing randomly mutated light chain CDR3 to generate Ab417. The affinities ( $K_D$ ) of Ab417 for human and mouse L1CAM were 0.24 nM and 79.16 pM, respectively. Ab417 specifically bound the Ig5 domain of L1CAM and did not exhibit off-target activity, but bound to the peripheral nerves embedded in normal human tissues as expected in immunohistochemical analysis. In a pharmacokinetics study, the mean half-life of Ab417 was 114.49 h when a single dose (10 mg/kg) was intravenously injected into SD rats. Ab417 significantly inhibited tumor growth in a human cholangiocarcinoma xenograft nude mouse model and did not induce any adverse effect in *in vivo* studies. Thus, Ab417 may have potential as an anticancer agent.

**Abbreviations:** L1CAM, L1 cell adhesion molecule; mAb, monoclonal antibody; Ig, immunoglobulin; Fn, fibronectin; scFv, single-chain variable fragment; FACS, fluorescence-activated cell sorting; CDR, complementarity-determining region; Fab, fragment antigen-binding;  $K_D$ , dissociation constant; ELISA, enzyme-linked immunosorbent assay; MACS, magnetic-activated cell sorting; hFc, human IgG1 Fc; ECD, extracellular domain; C $\gamma$ 1, heavy chain constant region 1; C $\kappa$ , light chain (kappa) constant region; PBS, phosphate-buffered saline; PBA, PBS containing BSA; VH, variable heavy chain; VL, variable light chain; TBST, tris-buffered saline containing Tween-20; IR, tumor growth inhibition rate; ANOVA, analysis of variance.

### ARTICLE HISTORY

Submitted 02 September 2015  
Revised 19 November 2015  
Accepted 20 November 2015


### KEYWORDS

Affinity maturation; cancer; human monoclonal antibody; L1CAM; phage display; yeast display

## Introduction


L1 cell adhesion molecule (L1CAM, CD171) is a 200–220 kDa transmembrane glycoprotein consisting of 6 immunoglobulin (Ig)-like domains followed by 5 fibronectin-type III repeats, a transmembrane domain, and a short cytoplasmic tail.<sup>1</sup> L1CAM was first described as a neural cell adhesion molecule and has been shown to initiate a variety of dynamic motile processes, including cerebellar cell migration and neurite outgrowth during central nervous system development.<sup>2</sup> L1CAM is expressed

to some extent in other normal cells, including lymphoid and myelomonocytic cells, kidney tubule epithelial cells, and intestinal crypt cells,<sup>3–5</sup> but is aberrantly expressed in a variety of malignant tumors. The expression of L1CAM in tumors is associated with poor prognosis and metastasis.<sup>6</sup> L1CAM promotes many cellular activities via homophilic interactions with its extracellular region<sup>1</sup> and heterophilic interactions with other CAMs, extracellular matrix molecules, signaling receptors, and

**CONTACT** Hyo Jeong Hong  [hjhong@kangwon.ac.kr](mailto:hjhong@kangwon.ac.kr)

\*Current address: Molecular Imaging and Therapy Branch, National Cancer Center, Goyang, Korea

\*\*Current address: Scripps Korea Antibody Institute, Chuncheon, Korea

 Supplemental material data for this article can be accessed on the publisher's website.

Published with license by Taylor & Francis Group, LLC © Seulki Cho, Insoo Park, Haejung Kim, Mun Sik Jeong, Mooney Lim, Eung Suk Lee, Jin Hong Kim, Semi Kim, and Hyo Jeong Hong

This is an Open Access article distributed under the terms of the Creative Commons Attribution-Non-Commercial License (<http://creativecommons.org/licenses/by-nc/3.0/>), which permits unrestricted non-commercial use, distribution, and reproduction in any medium, provided the original work is properly cited. The moral rights of the named author(s) have been asserted.

integrins.<sup>7-10</sup> The 4 N-terminal Ig-like domains (Ig1-4) mediate L1CAM homophilic binding.<sup>11,12</sup> Ig6 has an Arg-Gly-Asp (RGD) motif that binds to integrins,<sup>13</sup> whereas Fn3 binds to the fibroblast growth factor receptor.<sup>14</sup> L1CAM has been shown to enhance the proliferation, survival, motility, and apoptosis resistance of tumor cells in several types of cancers.<sup>15-22</sup> Furthermore, recent studies have implicated the involvement of L1CAM in tumor angiogenesis and immune evasion through the enrichment of immunosuppressive T cells in pancreatic cancer models.<sup>23,24</sup>

Monoclonal antibodies (mAbs) targeting tumor cells via growth factor receptors, such as HER2/neu or epidermal growth factor receptor, are clinically effective for the treatment of metastatic breast cancer or colorectal and head and neck cancers, respectively.<sup>25-28</sup> In studies with anti-L1CAM mAbs, a murine mAb significantly reduced tumor growth in pancreatic and ovarian carcinoma xenograft models, whereas a chimeric antibody reduced tumor growth in a cholangiocarcinoma xenograft model.<sup>29-31</sup> The results suggest that these anti-L1CAM mAbs have potential as anticancer agents for the treatment of cancer. However, the mAbs bind only to human L1CAM; thus, their pharmacokinetic and toxicological properties and therapeutic efficacy in mice models are different from those in humans. In addition, because L1CAM is expressed in neural cells and other normal cells, such as monocytes and kidney tubule epithelial cells, anti-L1CAM antibody use has safety concerns. Therefore, the generation of a mAb that cross-reacts with rodent L1CAM is necessary to validate its druggability in the earliest stages of antibody development.

In vitro technologies that display recombinant antibody libraries on the surface of phage or yeast have been used to produce antibodies with high affinity and specificity and to improve biophysical properties.<sup>32-34</sup> Naïve, immune, semi-synthetic, and synthetic antibody libraries have been constructed in single-chain variable fragment (scFv) or Fab format.<sup>35</sup> The major advantages of phage display include application to a wide range of antigens, irrespective of their immunogenicity and toxicity, the isolation of cross-reactive antibodies for animal models, and the ability to fully control the selection conditions.<sup>36</sup> Yeast display is more useful for affinity maturation than other in vitro display technologies, as it allows quantitative screening and compensation of the antigen-binding signal to expression signal during fluorescence-activated cell sorting (FACS).<sup>37</sup>

Cholangiocarcinoma is a malignant tumor arising from the bile duct epithelium. The prognosis for cholangiocarcinoma is poor due to the lack of early diagnosis and because it is refractory to conventional chemotherapy and radiation therapy.<sup>38</sup> A Phase 3 clinical trial in advanced biliary cancers reported significant prolongation of median overall survival when gemcitabine is combined with cisplatin compared to gemcitabine alone, establishing this combination as a global standard of care.<sup>39</sup> However, the 5-year survival of cholangiocarcinoma remains low.<sup>40</sup> Therefore, targeted therapies that improve patient survival are needed for patients with advanced biliary cancer. Previously, we found that L1CAM is aberrantly expressed in cholangiocarcinoma and plays an important role in tumor progression by enhancing cell proliferation, migration, apoptosis resistance, and tumor growth.<sup>18,19,22,41,42</sup> Here, we isolated a human anti-L1CAM mAb that binds to human and mouse L1CAM from a human naïve

Fab library using phage display and developed an affinity-matured antibody (Ab417) through site-directed mutagenesis of complementarity-determining regions (CDR) residues and yeast display of scFvs containing randomly mutated light chain CDR3. Subsequently, we evaluated the specificity, pharmacokinetic properties, and anti-tumor efficacy of Ab417 in rodent models.

## Results

### *Isolation of human Fabs binding human and mouse L1CAM from phage-displayed antibody library*

To isolate human mAbs that bind to both human and mouse L1CAM, a human naïve Fab library was screened by panning against the extracellular domains of human and mouse L1CAM. The first and second rounds of panning were performed against human L1CAM, and the third panning was performed against mouse L1CAM. Finally, 6 different cross-reactive Fab clones were obtained, with Ab4 Fab having the highest antigen binding activities to both human and mouse L1CAM. This clone was selected for further study. Ab4 Fab was converted to human IgG1 form (Ab4), expressed transiently in HEK293T cells, and then purified by affinity chromatography on a Protein A column. The affinity ( $K_D$ ) of Ab4 for human L1CAM by competitive ELISA was approximately 100 nM (data not shown).

### *Affinity maturation of Ab4 by site-directed mutagenesis*

For affinity maturation of Ab4, we performed alanine-scanning mutagenesis on the HCDR1, HCDR2, HCDR3, and LCDR3 residues to analyze the role of each residue in antigen binding. As shown in Fig. 1A, alanine mutation (H97A) of His97 in HCDR3 increased the antigen-binding activity for human and mouse L1CAM, whereas the mutation of other residues in HCDR1, HCDR2, and HCDR3 significantly decreased the binding activity for human L1CAM. In the case of LCDR3, alanine mutation (D93A) of Asp93 increased the activity, but the mutation of other residues did not (Fig. 1B). We also mutated Val50 in HCDR2 to glutamate, phenylalanine, tyrosine, arginine, or threonine. Because alanine mutation (V50A) of Val50 moderately decreased the activity, the valine residue was speculated to be involved in antigen binding, but to not be optimal for antigen binding. Substitution of glutamate or phenylalanine for valine increased the binding activity for human L1CAM (Fig. 1C). Consequently, we constructed a variant (Ab4M) of Ab4 that contains 3 mutations (V50F in HCDR2, H97A in HCDR3, and D93A in LCDR3) and compared its affinity to that of Ab4 by competitive ELISA. The affinities ( $K_D$ ) of Ab4 and Ab4M for human L1CAM were 130 nM and 2.9 nM, respectively, whereas those of the mutants carrying D93A, H97A, or V50F and H97A were 28 nM, 23 nM, or 16 nM, respectively (Fig. 2A). The results indicate that the affinity of Ab4M for human L1CAM was increased 44-fold compared to that of Ab4 due to the synergistic effect of the 3 critical mutations.

### *Epitope mapping and cross-reactivity of affinity-matured antibody (Ab4M)*

For epitope mapping of Ab4M, the antibody was subjected to Western blot analysis using truncated extracellular domains of

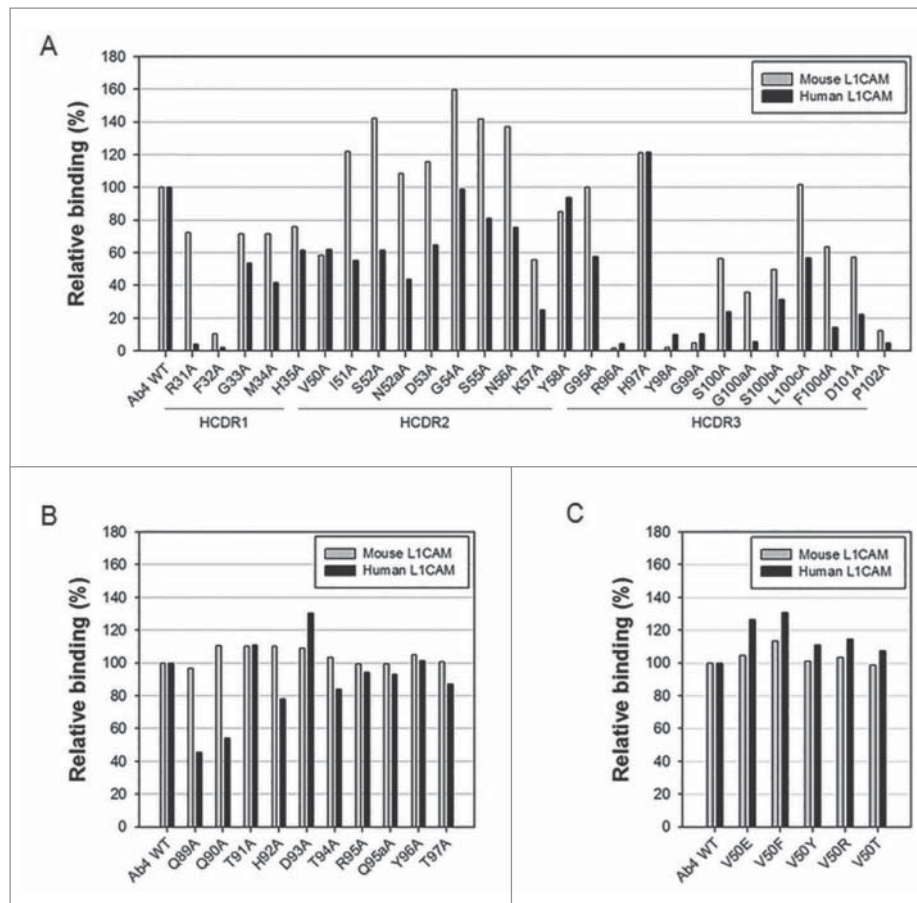


**Figure 1.** Antigen-binding activities of Ab4 mutants for human (black bars) and mouse (gray bars) L1CAM. Each mutant with alanine replacement in the HCDRs (A) or LCDR3 (B) or other mutation at Val50 in the HCDR2 (C) was subjected to indirect ELISA. Relative binding percentage of each mutant compared to Ab4 is shown.

human L1CAM fused to human Fc (hFc).<sup>43</sup> Ab4M bound to Ig5, Ig1-5, and Ig1-6, but did not bind to Ig1-4, Ig6, or Fn1-5, indicating that Ab4M binds to Ig5 (Fig. 2B).

To confirm the cross-reactivity of Ab4M with L1CAM from other species, Ab4M was subjected to Western blot analysis using brain tissues from rat, dog, and cynomolgus monkey, as well as recombinant human and mouse L1CAM proteins as positive controls. As shown in Fig. 2C, Ab4M reacted with 2 bands of L1CAM from the tested tissues, consistent with previous reports.<sup>2,5</sup> In addition, we confirmed the reactivity with mouse and rat L1CAM by flow cytometric analysis using rat PC12 and mouse melanoma B16F1 cells.

#### Affinity maturation of Ab4M by yeast display

Yeast display technology was employed to improve the affinity of Ab4M. First, the scFv form of Ab4M was displayed on the surface of yeast and its antigen-binding activity was measured by flow cytometric analysis using different concentrations of L1CAM (Fig. S1A). Next, 7 residues (amino acids 90-96) in the LCDR3 of Ab4M scFv were randomized to construct a  $2 \times 10^9$  sub-library, which was then screened by magnetic activated cell sorting (MACS) with  $1 \times 10^{-7}$  M antigen followed by 2 rounds of FACS with  $5 \times 10^{-9}$  M antigen. A total of  $3 \times 10^3$  colonies were obtained from cell sorting. Finally, 48 clones were recovered and the antigen-binding signal to cell-surface

expression signal was analyzed by flow cytometry. One clone with the highest antigen-binding activity was selected (Fig. S1B) and converted into human IgG1 form. This antibody was named Ab417.

#### Affinity determination with Ab417

The affinities ( $K_D$ ) of Ab4, Ab4M, and Ab417 for human and mouse L1CAM were measured by competitive ELISA. The affinities of Ab4, Ab4M, and Ab417 for human L1CAM were  $1.3 \times 10^{-7}$  M,  $2.9 \times 10^{-9}$  M, and  $1.2 \times 10^{-9}$  M, respectively (Fig. 3A), whereas the affinities for mouse L1CAM were  $1.7 \times 10^{-9}$  M,  $2.2 \times 10^{-10}$  M, and  $2.1 \times 10^{-10}$  M, respectively (Fig. 3B). Thus, the affinity of Ab417 for human L1CAM was increased 2.4-fold compared to Ab4M, but the affinity for mouse L1CAM was similar to that of Ab4M. One explanation for this finding is that Ab4 already had a high affinity for mouse L1CAM and the affinity of Ab4M was further increased 7.7-fold compared to Ab4; thus, the high affinities of Ab4M and Ab417 for mouse L1CAM may not have been measured accurately by competitive ELISA because of the limitation of this method.

The antigen-binding kinetics of Ab417 and Ab4M for human and mouse L1CAM were determined using the Octet<sup>®</sup> RED System (Fig. S2). The affinities ( $K_D$ ) of Ab417 and Ab4M for human L1CAM were 0.24 nM and 0.43 nM, respectively, whereas the affinities for mouse L1CAM were 79.16 pM and 0.14 nM, indicating that the affinities of Ab417 for both human

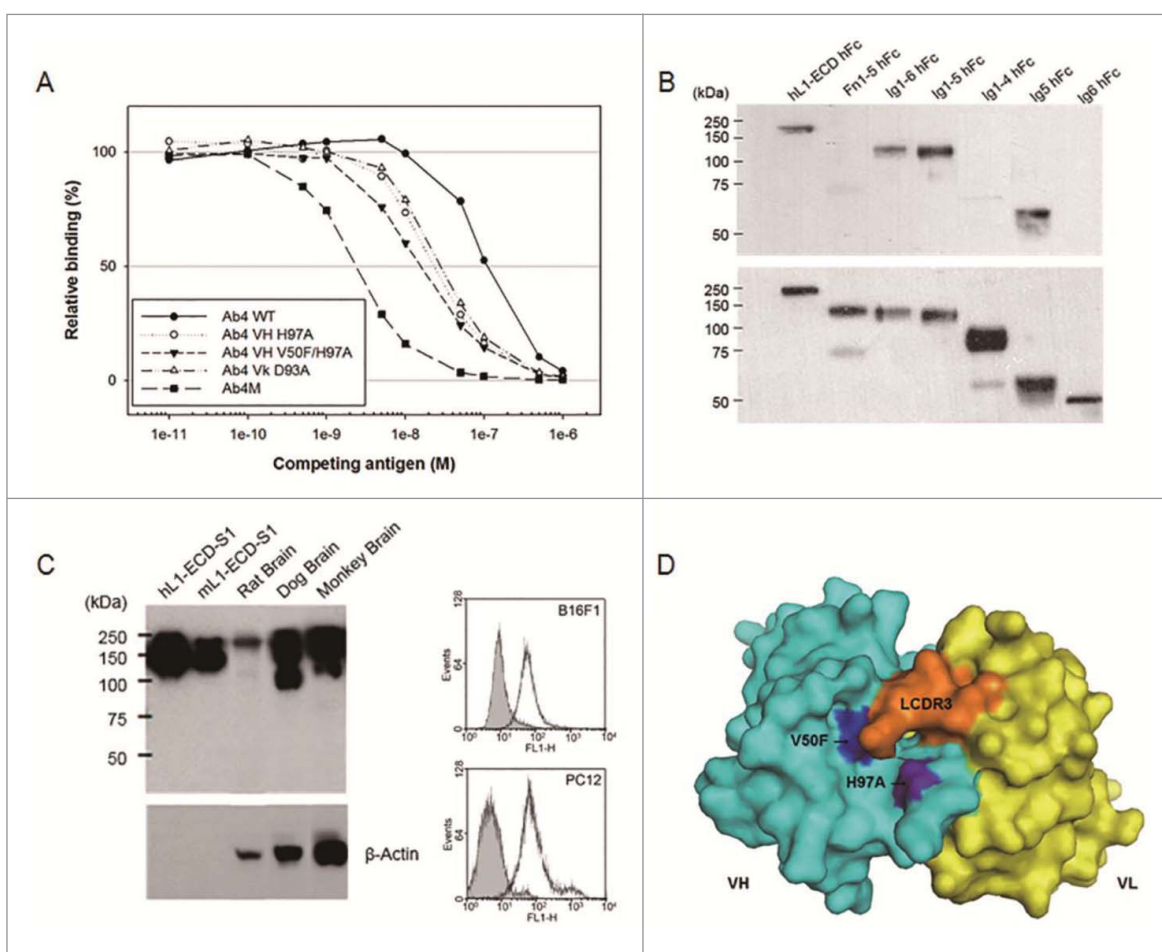


**Figure 2.** Affinity (A), epitope mapping (B), cross-reactivity (C) of Ab4M, and a structural model of Ab417 Fv (D). (A) Affinities of Ab4, Ab4 mutants (H97A, V50F plus H97A, and D93A) and Ab4M for human L1CAM were determined by competitive ELISA. (B) Serially truncated mutants of human L1CAM fused to hFc were subjected to Western blot analysis using Ab4M and anti-human Fab-HRP (top) or anti-hFc-HRP (bottom). (C) Homogenized brain tissues of animals (rat, dog, cynomolgus monkey) and purified human (hL1-ECD-S1) and mouse (mL1-ECD-S1) L1CAM proteins were subjected to Western blot analysis using Ab4M or anti- $\beta$ -actin antibody. (D) Upside view of 3D model of Ab417 Fv. The V50F, H97A, and LCDR3 that contributed to affinity maturation are indicated. Cyan, VH; yellow, VL; blue, V50F mutation; purple, H97A mutation; and orange, LCDR3.

and mouse L1CAM were increased 1.8-fold compared to those of Ab4M (Fig. 3C). The increased affinity of Ab417 compared to Ab4M was due to the slower dissociation rate. The two HCDR residues and changed LCDR3 that contributed to the affinity maturation of Ab4 are presented in the structural model of Ab417 Fv (Fig. 2D). Because the affinities of Ab417 for human and mouse L1CAM are high enough to characterize in vivo profiles, we considered Ab417 as the final candidate for preclinical study.

### Specificity of Ab417

The antigen-binding specificity of Ab417 was confirmed by indirect ELISA using several truncated domains of human L1CAM. Ab417 bound to Ig5-hFc and Ig1-5-hFc with high affinity but did not bind to Ig1-4-hFc and Ig6-Fn5-hFc (Fig. 4A), demonstrating that Ab417 binds specifically to the Ig5 domain.

The binding specificity of Ab417 was also analyzed using a protein microarray of 384 extracellular, secretory, membrane, and intracellular human proteins (Fig. 4B) with human L1CAM as a positive control. Ab417 reacted with L1CAM but did not bind to any protein in the microarray, suggesting that Ab417 does not have off-target activities.

Next, to examine the normal tissue cross-reactivity of Ab417, we performed immunohistochemistry using 10 types of normal human tissue (cerebellum, adrenal gland, gastrointestinal tract, liver, lung, ovary, pancreas, spleen, thyroid, and uterus) and L1CAM-expressing cholangiocarcinoma cells (SCK)<sup>22</sup> as a positive control. The cerebellum and adrenal gland express L1CAM at high and medium levels, respectively, whereas the other tissues do not express L1CAM based on RT-PCR and immunohistochemical analysis.<sup>44</sup> Consistently, Ab417 strongly reacted with the cerebellum and weakly with the adrenal gland but did not react with the other 8 normal tissues (data not shown); however, it bound to L1-CAM expressing peripheral nerves embedded in the tissues, as evidenced in the ovarian tissue (Fig. 4C).

### Single-dose pharmacokinetics of Ab417 in rats

Because Ab417 binds rat L1CAM, the pharmacokinetic properties of Ab417 were assessed in rats. Antibody was produced from a stable Chinese hamster ovary (CHO) cell line. We produced recombinant rat L1-ECD-S1 and performed Octet kinetics assay to accurately measure the affinity ( $K_D$ ) of Ab417 for rat L1CAM, which was shown to be 98.4 pM (Fig. S3), similar

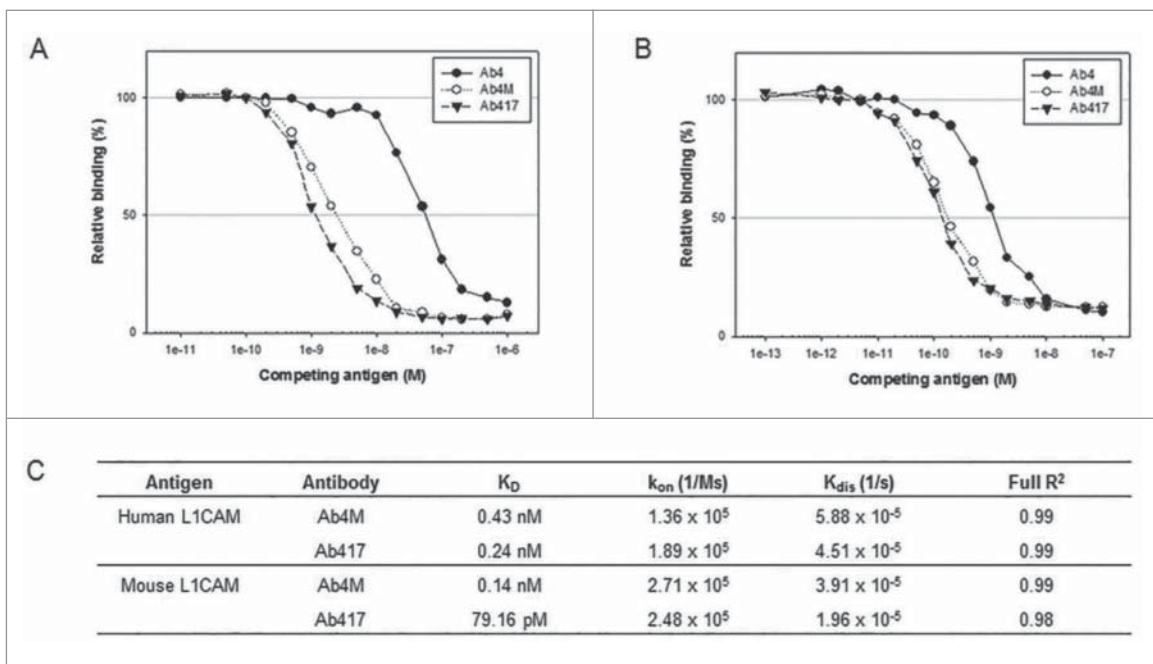


**Figure 3.** Affinity determination of Ab4, Ab4M, and Ab417 for hL1-ECD-S1 (A) and mL1-ECD-S1 (B) by competitive ELISA and Octet Red system (C).  $k_{on}$ , rate of association;  $k_{dis}$ , rate of dissociation; and Full  $R^2$ , an estimate of the goodness of the curve fit.

to that (79.16 pM) for mouse L1CAM. A single dose of 3 or 10 mg/kg antibody was intravenously (i.v.) injected into 3 male Sprague-Dawley (SD) rats and blood samples were taken at 1, 6, 12, 24, 48, 72, 120, 168, and 240 h. The serum concentrations of the antibody were measured by indirect ELISA using recombinant human L1CAM as a coating antigen. The pharmacokinetic profile and parameters are shown in Fig. 5. The antibody concentration after 3 mg/kg injection declined slightly faster than the concentration after 10 mg/kg injection, and at 240 h the serum concentration was 2.3 and 12.7  $\mu\text{g}/\text{mL}$  after 3 and 10 mg/kg injection, respectively. With the 10 mg/kg dose, the area under the plasma concentration-time curve extrapolated to the last sampling point ( $AUC_{last}$ ), the maximum observed plasma concentration ( $C_{max}$ ), and mean half-life ( $t_{1/2}$ ) were  $8,604.50 \pm 1,111.35 \mu\text{g}\cdot\text{h}/\text{mL}$ , 204  $\mu\text{g}/\text{mL}$ , and  $114.49 \pm 10.23$  h, respectively, whereas the total body clearance ( $CL_t$ ) was 0.94 mL/h/kg. The  $AUC_{last}$ ,  $C_{max}$ , and  $t_{1/2}$  increased 2.5, 2.3, and 1.7-fold, respectively, with the 10 mg/kg dose compared to 3 mg/kg, whereas  $CL_t$  increased little. The data suggest that the  $CL_t$  of Ab417 comprises an antigen-mediated clearance component and a non-specific clearance component, with a greater contribution of the antigen-mediated clearance component with the 3 mg/kg dose. No general toxicities were observed in the animals.

#### **In vivo anti-tumor activity of Ab417 in cholangiocarcinoma xenograft nude mouse model**

The anti-tumor efficacy of Ab417 was evaluated in the L1CAM-expressing human cholangiocarcinoma Choi-CK xenograft nude mouse model. The anti-L1CAM chimeric antibody (cA10-A3) we previously developed was included as a reference because it demonstrated tumor growth inhibition in the same xenograft model, but its affinity is 10-fold lower than Ab417

and it lacks cross-reactivity with mouse L1CAM.<sup>31</sup> Ab417 or cA10-A3 at 10 mg/kg or hFc at 3.3 mg/kg was i.v. injected thrice a week into nude mice bearing a Choi-CK xenograft. The tumor volume and body weight of the mice were measured for 3 weeks. At 22 days post-injection, tumor tissues were removed and weighed. The Ab417-treated groups had a mean tumor volume of 320  $\text{mm}^3$  ( $p < 0.01$ ) and tumor weight of 0.219 g ( $p < 0.05$ ), whereas cA10-A3-treated groups had a mean tumor volume of 722  $\text{mm}^3$  and tumor weight of 0.649 g ( $p < 0.05$ ) (Fig. 6A and 6B). Based on tumor weight, Ab417 resulted in 68.6% tumor growth inhibition compared to hFc without affecting body weight, whereas cA10-A3 resulted in 22.5% tumor growth inhibition. No general toxicities were observed in the control or treated mice, and the mice treated with Ab417 had increased weight compared to those treated with cA10-A3 (Fig. 6C). Thus, the results clearly demonstrate that Ab417 has higher antitumor activity than cA10-A3.

#### **Discussion**

In this study, we generated a human mAb that cross-reacts with mouse L1CAM using phage display and increased its affinity by site-directed mutagenesis and yeast display. The resulting antibody, Ab417, had high affinities ( $K_D$ ) for human and mouse L1CAM and did not exhibit any off-target activity. At a single dose of 10 mg/kg, the antibody had a fairly long serum half-life in SD rats but did not induce any general toxicities. In addition, the antibody exhibited significantly higher antitumor activity than cA10-A3 in a cholangiocarcinoma xenograft model and did not induce any adverse effects, even after being injected thrice weekly for 3 weeks. The results suggest that Ab417 has potential as a therapeutic agent for the treatment of L1CAM-positive cancers. To the best of our knowledge, Ab417 is the first fully human anti-L1CAM mAb.

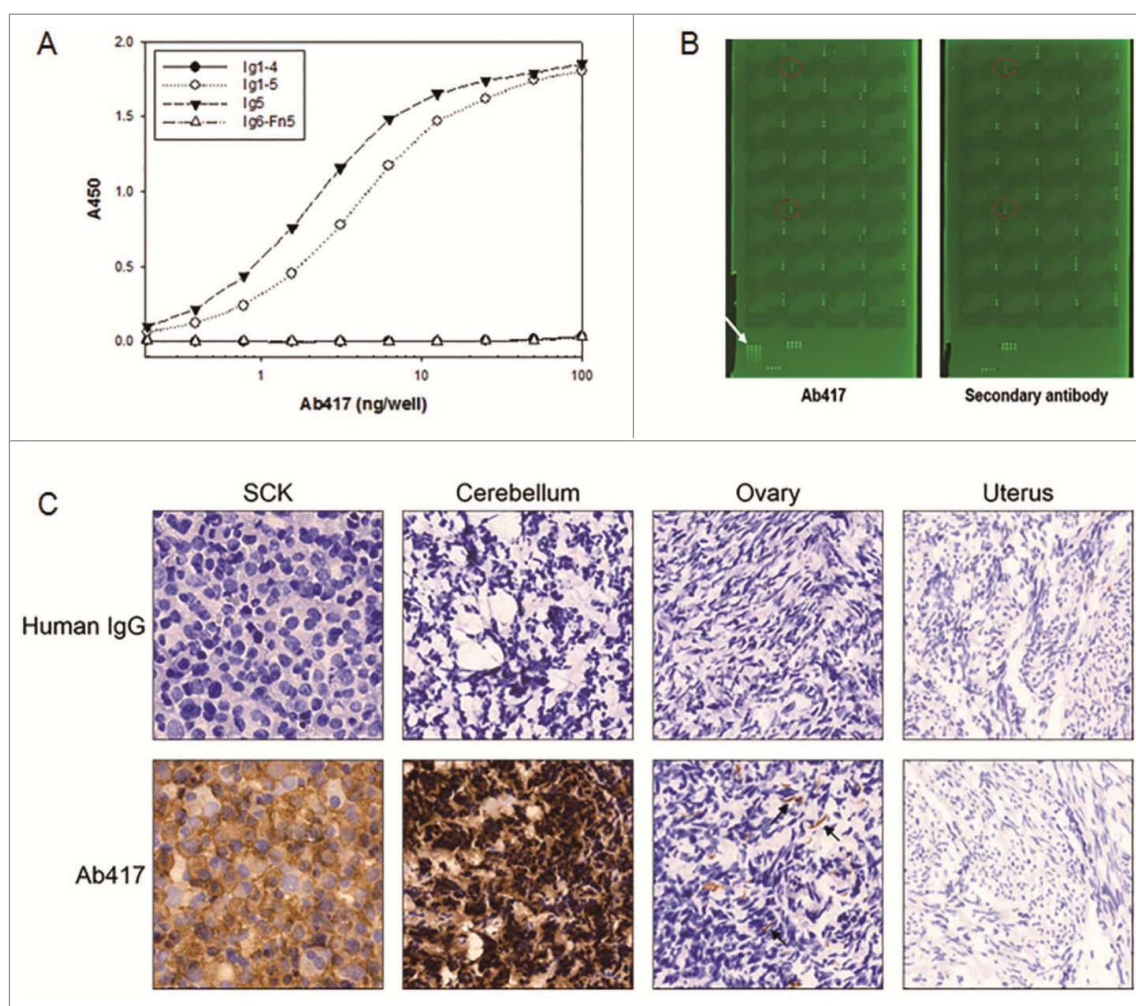


**Figure 4.** Specificity of Ab417. (A) Epitope of Ab417 was confirmed by indirect ELISA using Ig1-4, Ig1-5, Ig5, and Ig6 through Fn1-5 (Ig6-Fn5). (B) Off-target activity of Ab417 was analyzed using UNichip<sup>®</sup> AV-400 protein microarray with human L1CAM used as a positive control. Ab417 bound to the L1CAM up to the signal intensity of 154% (white arrow) with no off-target activity. Red circle indicates the secondary antibody control. (C) Normal tissue cross-reactivity of Ab417 or human IgG as a negative control was analyzed by immunohistochemistry using 10 types of human normal tissues and L1CAM-expressing tumor cells (SCK) as a positive control. Ab417 bound to the SCK cells and the cerebellum that was reported to express L1CAM but did not bind to other tissues (for example, ovary and uterus). The arrow in the ovary sample indicates the peripheral nerves stained by Ab417.

In addition, Ab417 has advantages over previous anti-L1CAM mAbs due to high affinity, better therapeutic efficacy, and cross-reactivity with rodent L1CAM, which may facilitate its preclinical and clinical development.

Epitope mapping experiments revealed that Ab417 binds to the Ig5 domain of L1CAM. Because Ab417 cross-reacts with L1CAM from mouse, rat, dog, and cynomolgus monkey, its epitope sequence may be evolutionarily conserved.<sup>44</sup> Murine anti-L1CAM mAbs generated by immunizing mice with human L1CAM protein have been shown to recognize the Ig1, Ig3, or Fn4 domain,<sup>30,43,45,46</sup> but a mAb binding the Ig5 domain has not been reported. This may be due to higher sequence homology (92%) of Ig5 between humans and mice, compared to sequence homology (88%) of entire L1CAM sequence.<sup>44</sup> This study demonstrates the advantages of phage display technology in generating rodent-cross-reactive antibodies. To our knowledge, Ab417 is the only mAb specific to the Ig5 of L1CAM.

Studies on the functions of L1CAM have shown that the Ig1-4 domains mediate homophilic interactions with other L1CAM in *trans* and enhanced proliferation of cancer cells

by activating ERK1/2 signaling, whereas an Ig6 domain-containing RGD motif bound to integrins and enhanced cell motility and invasiveness via the NF- $\kappa$ B signaling pathway.<sup>47</sup> However, the function of the Ig5 domain is unknown. Ab417 did not inhibit the proliferation of tumor cells in vitro, but it exhibited excellent tumor growth inhibition in vivo. The same phenomenon was observed in another study with anti-L1CAM mAb recognizing the Ig1 domain and inhibiting tumor growth in ovarian carcinoma xenograft nude mouse models.<sup>29-31,46</sup> The mode of action of Ab417 will be elucidated in a future study.

L1CAM expression in the peripheral nerves and kidney tubules raises concerns that anti-L1CAM mAb may induce toxicity. In this study, Ab417 did not induce any adverse effect in the pharmacokinetics and efficacy studies. In addition, when Ab417 (30  $\mu$ g/mL) was directly added to human neural progenitor cells, ReNcell VM,<sup>48</sup> it did not affect the cells (data not shown). A repeated-dose toxicological study of Ab417 in cynomolgus monkeys remains to be conducted to predict potential toxicity in humans.

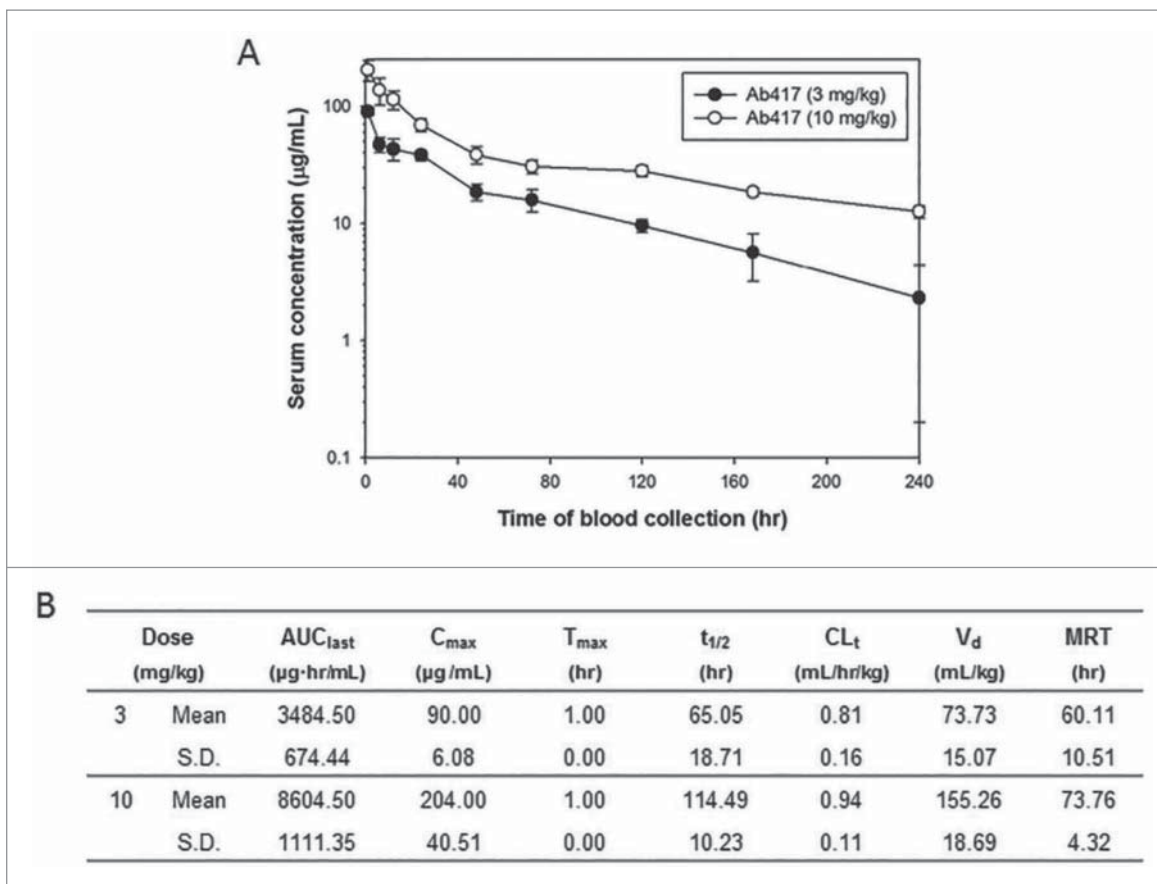


**Figure 5.** Pharmacokinetics of Ab417 in SD rats. (A) Serum concentration of Ab417 relative to time profiles after single intravenous administration. Concentration of antibodies in rat plasma was assessed by indirect ELISA against human L1CAM. Each bar represents the mean  $\pm$  SD,  $n = 3$ . (B) Mean data of PK parameters. SD, standard deviation; AUC<sub>last</sub>, the area under the plasma concentration-time curve extrapolated to the last sampling point; C<sub>max</sub>, the maximum observed plasma concentration; T<sub>max</sub>, the time of occurrence of C<sub>max</sub>; t<sub>1/2</sub>, the apparent terminal half-life; CL<sub>t</sub>, total body clearance; MRT, mean residence time; and V<sub>d</sub>, distribution volume.

In summary, we successfully developed a high affinity human anti-L1CAM mAb (Ab417) that cross-reacts with rodent L1CAM using phage display and yeast display technologies in combination with site-directed mutagenesis. Ab417 had a long serum half-life in rats and good anti-tumor efficacy in a cholangiocarcinoma xenograft nude mouse model. No general toxicities were observed in the *in vivo* studies. Therefore, Ab417 may have potential as a therapeutic agent for the treatment of cholangiocarcinoma and other types of L1CAM-positive cancers.

## Materials and methods

### Cell lines and cell culture

HEK293T, Choi-CK, SCK, PC12, and B16F1 cells were grown at 5% CO<sub>2</sub>, 37°C in DMEM (Welgene, Republic of Korea) supplemented with 10% FBS (Atlas). CHO-DG44 cells<sup>49</sup> were grown at 5% CO<sub>2</sub>, 37°C in MEM- $\alpha$  (Welgene) supplemented with 5% (v/v) dialyzed FBS (Gibco).

### Selection of Fabs binding to human and mouse L1CAM from a phage antibody library

Human combinatorial naïve Fab library was constructed as described previously.<sup>50</sup> For preparation of the panning antigens, the extracellular domain (ECD) of human L1CAM (hL1-ECD) was expressed in HEK293T cells and purified from the

culture supernatant by affinity chromatography on a protein A-sepharose column (Millipore) conjugated with anti-L1CAM mAb, A10-A3.<sup>18</sup> Also, the ECD (mL1-ECD-S1) of mouse L1CAM fused to the preS1 tag<sup>51</sup> at its C-terminus was expressed and purified by affinity chromatography on a sepharose column conjugated with anti-preS1 mAb, KR127, as described previously.<sup>31</sup> Phage-displayed human naïve Fab library was prepared using VCSM13 helper phages and panned against hL1-ECD for the first and second rounds followed by mL1-ECD-S1 for the third round, using the standard protocols.<sup>52</sup> After panning, *E. coli* TG1 cells were infected with the eluted phages and cultured in 2xYT medium (2  $\times$  YTA) containing ampicillin overnight. Total 125 colonies were chosen randomly, separately inoculated into 2  $\times$  YTA media and incubated at 37°C until the OD600 reached to 0.7. Subsequently, 1 mM IPTG was added to the culture and expression of soluble Fab fused to Protein III was induced at 30°C overnight. The culture supernatant was subjected to indirect ELISA, quantitative ELISA, and competitive ELISA to select high-affinity clones for both human and mouse L1CAM.

### Conversion of Fabs into IgG1 format and expression of IgG1

To convert the selected Fabs into whole IgG1, the human VH and V $\kappa$  sequences were amplified by PCR and

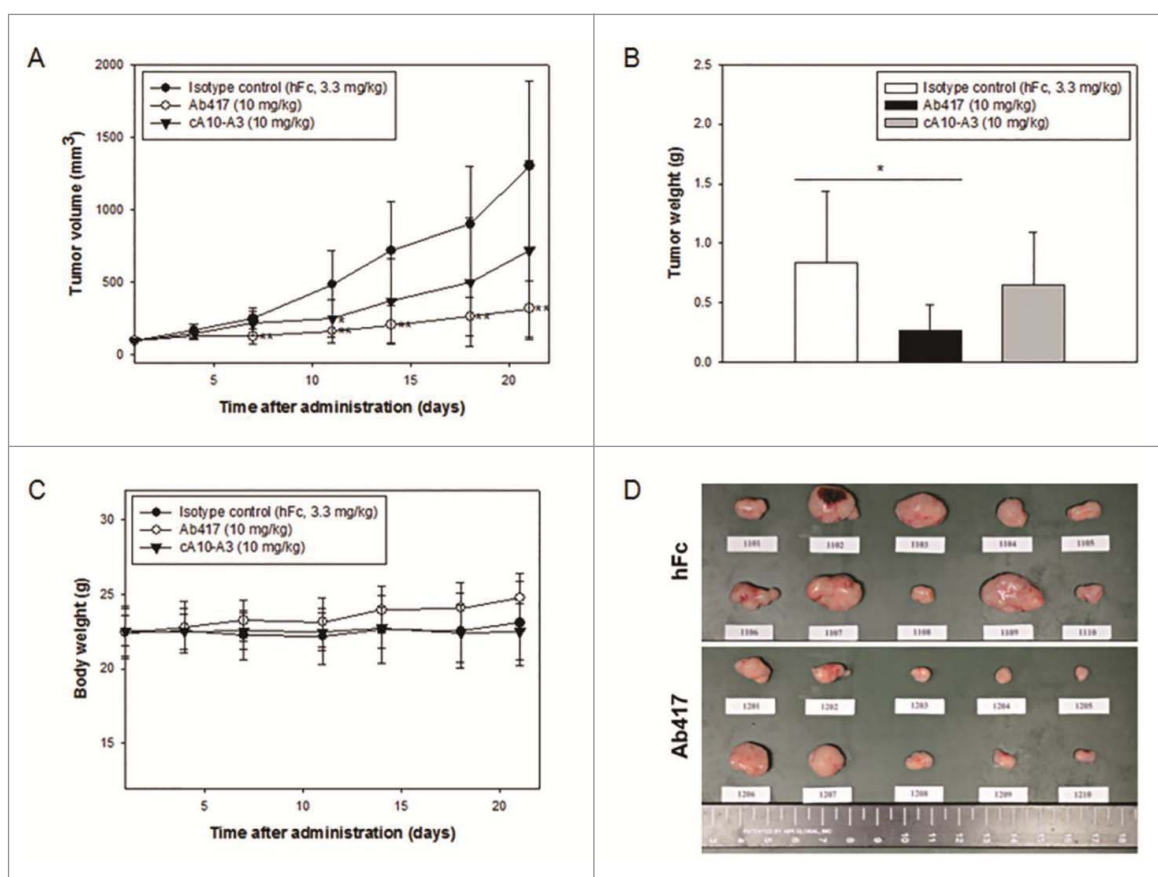


**Figure 6.** Anti-tumor efficacy of Ab417 in comparison with cA10-A3 in Choi-CK cholangiocarcinoma xenograft model. Ab417, cA10-A3, or hFc as an isotype control was i.v. injected into nude mice ( $n=10$  per group) thrice a week for 21 days. Mean tumor volume (A), tumor weight (B), and body weight (C) are shown. Each point represents the mean  $\pm$  SD; bars, SD; \* $p < 0.05$ , \*\* $p < 0.01$ , significant difference from the isotype control group by Dunnett's t-test. (D) Photographs of the resected tumors at the end of experiment.

combined with the leader sequences of IgG heavy and light chains, respectively, by recombinant PCR. The resulting VH and V $\kappa$  were sequentially subcloned into the *EcoRI-ApaI* and *HindIII-BsiWI* sites, respectively, in the expression plasmid (pdCMV-*dhfrC*) containing the human C $\gamma$ 1 and C $\kappa$  gene.<sup>53</sup> The IgG1 expression plasmid was introduced into HEK293T cells using polyethylenimine (Polysciences) according to the Cold Spring Harbor Protocols, and the transfected cells were cultured in protein-free medium (CD293, Invitrogen or Pro-293a CDM, Lonza). The culture supernatant was centrifuged and filtered using a bottle top filter (0.22  $\mu$ m PES, Sartorius), and then subjected to quantitative ELISA and indirect ELISA to analyze antigen binding affinity. IgG1 was purified from the culture supernatant by affinity chromatography on a protein A-agarose (Millipore), and the protein concentration was determined with a NanoDrop (Thermo Scientific).

### ELISAs

Indirect ELISA was carried out using hL1-ECD-S1 or mL1-ECD-S1 (100 ng/well) as a coating antigen, as described previously.<sup>31</sup> For competitive ELISA, 0.1% PBA (PBS containing 0.1% BSA) solution containing antibody (1.5–5.9  $\mu$ g/mL) and various concentrations ( $10^{-11}$ – $10^{-6}$  M) of hL1-ECD-S1 or mL1-ECD-S1 as a competing antigen were pre-incubated at

37°C for 3 h. The mixture was then added to each well, which had been coated with 100 ng of hL1-ECD-S1 or mL1-ECD-S1. Bound antibody was detected by indirect ELISA. Affinity was determined as the antigen concentration required to inhibit 50% of binding activity and  $K_D$  value was calculated from a Klotz plot.

### Western blot analysis

For epitope mapping of Ab4M, hL1-ECD and its truncated domains fused to hFc<sup>43</sup> were expressed in HEK293T cells and the culture supernatant containing 5  $\mu$ g of each protein sample was reduced and subjected to 10% SDS-PAGE and protein bands were transferred to nitrocellulose membrane. After blocking with TBST (TBS containing 0.1% Tween-20) containing of 5% skim milk (BD), the membrane was incubated with Ab4M (0.3  $\mu$ g/mL), followed by anti-human IgG F(ab')<sub>2</sub>-HRP conjugate (1:5,000, v/v, Thermo Scientific) or incubated with anti-human IgG(Fc-specific)-HRP conjugate (1:10,000 v/v, Thermo Scientific).

For cross-reactivity study of Ab4M, brain tissues obtained from rat, dog, and monkey were homogenized and together with purified hL1-ECD-S1 and mL1-ECD-S1 were subjected to 10% SDS-PAGE and Western blot analysis using Ab4M, followed by anti-human IgG-HRP conjugate (1:15,000, v/v, Thermo Scientific).  $\beta$ -Actin was detected using rabbit anti-



$\beta$ -Actin mAb (1:1,000, Cell Signaling) and goat anti-rabbit IgG-HRP (1:5,000, Santa Cruz Biotechnology).

### Flow cytometry

B16F1 or PC12 cells ( $2 \times 10^5$ ) were incubated with Ab417 or human IgG (Thermo Scientific) as a negative control at 4°C for 1 h. After washing twice with 0.1% PBA, the cells were incubated with anti-human IgG (Fc-specific)-FITC (Sigma Aldrich) at 4°C for 1 h. Propidium iodide-negative cells was analyzed for antibody binding using FACSCalibur (Becton Dickinson), and data was analyzed by WinMDI ver. 2.9.

### Affinity determination of antibody by octet red system

Anti-hFc sensor (AHC, ForteBio) was first soaked in 0.1% PBA for 20 min, antibody (0.2 mL of 2  $\mu$ g/mL) was captured for 10 min, and then washed in 0.1% PBA for 2 min. Purified hL1-ECD (100, 50, 25, 12.5 and 6.25 nM) and mL1-ECD-S1 (30, 10, 3.3, and 1.1 nM) were prepared as a serial dilution in PBA and incubated with antibody bound on the chips. Association and dissociation rates were measured for 15 and 30 min, respectively. All measurements were corrected for baseline drift by subtracting a control sensor (antibody-captured AHC sensor) exposed to running buffer only. Operating temperature was maintained at 30°C. Data were analyzed using a 1:1 interaction model (fitting global, Rmax unlinked by sensor) with analysis software (ForteBio, ver. 7.1).

### Affinity maturation of Ab4M by yeast display

The gene encoding the Ab4M scFv was synthesized by PCR and subcloned into pYD1 plasmid (Invitrogen) to yield pYD1-scAb4M. This plasmid was introduced into yeast strain, EBY100. Display of the scFv on the surface of yeast cells and its antigen-binding activity were measured by flow cytometric analysis using different concentrations ( $10^{-5}$ – $10^{-8}$  M) of Ig5-hFc. Seven residues in the LCDR3 of Ab4M were randomized by PCR using hand-mixed XYZ (X contained 38% G, 19% A, 26% T and 17% C; Y contained 31% G, 34% A, 17% T and 18% C; and Z contained 24% G and 76% C) oligonucleotide<sup>54</sup> provided by IDT (USA) to construct a scFv sub-library. The resulting PCR products and the pYD1 digested with *SphI/EcoRI* were mixed to transform the yeast cells by electroporation. The transformants ( $2 \times 10^9$ ) were induced with galactose and incubated with Ig5-hFc ( $1 \times 10^{-7}$  M) for 1 h and subjected to MACS. Colonies ( $1.37 \times 10^7$ ) were recovered and incubated with Ig5-hFc ( $5 \times 10^{-9}$  M) for FACS on a FACSaria (Becton Dickinson), as described previously.<sup>37</sup> After cell sorting,  $3 \times 10^3$  cells were obtained and 48 viable colonies were subjected to DNA sequencing to determine their VH and VL sequences.

### Modeling of the 3-dimensional structure of Ab417

Structural models of Ab417 Fv were generated using Lonza's modeling platform. Candidate structural template fragments for the framework and CDRs as well as the full Fv were scored, ranked and selected from Lonza's antibody database based on their sequence identity to the target. In order to structurally align

the CDRs to the FR templates, 5 residues on either side of the CDR were included in the CDR template. An alignment of the fragments was generated based on overlapping segments and a structural sequence alignment. The template fragments along with the alignment were processed by MODELLER (Accelrys). This protocol creates conformational restraints derived from the set of aligned structural templates. An ensemble of structures that satisfy the restraints were created by simulated annealing and conjugate gradient optimization procedures. One or more model structures were selected from this ensemble on the basis of an energy score, derived from the score of the quality of the protein structure and satisfaction of the conformational restraints. The models were inspected and the side chains of the positions which differ between the target and template were optimized using a side chain optimization algorithm and energy minimized. A suite of visualization and computational tools were used to assess the conformational variability of the CDRs, as well as the core and local packing of the domains and regions and a surface analysis to select one or more preferred models.

### Construction of stable CHO cell line and production of Ab417

For large scale production of Ab417, the gene encoding the heavy or light chain was codon-optimized for mammalian cell expression and subcloned into the *EcoRI-NotI* or *HindIII-XbaI* site of pdCMV-*dhfrC*, respectively, to yield pdCMV-*dhfrC*-Ab417. This expression plasmid was introduced into CHO-DG44 cells, and stably transfected cell lines were selected in a medium containing G418 (550  $\mu$ g/mL). A subclone (#9) was adapted to 20 nM methotrexate (Sigma Aldrich) for gene amplification, and survived cells (#9-20) were grown in serum-free medium (SFM4CHO, Thermo Scientific). The culture supernatant was subjected to affinity chromatography on a protein A-agarose for purification, as described previously.<sup>31</sup>

### Off-target activity assay

UNIchip<sup>®</sup> Av-400 microarray (PROTAGEN, Germany) was blocked with 2% BSA in TBST (2% BSA/TBST) at room temperature and incubated with 0.05  $\mu$ M Ab417, followed by goat anti-human IgG F(ab')<sub>2</sub>-Cy3 (Protagen) in 2% BSA/TBST. Read out of the results was performed with a confocal microarray reader (ScanArray 4000, Perkin Elmer Life Science).

### Immunohistochemistry

Reactivity of Ab417 to normal human tissues was assessed by Reference Bio Laboratories Inc.. Tissue sections of 6  $\mu$ m thickness were cut and embedded in optimal cutting temperature (OCT) compounds. Sections were stained using avidin-biotin system followed by development with DAB chromogen (DakoCytomation, Carpinteria, CA). Human IgG was used as a negative control.

### Pharmacokinetics study of Ab417

Pharmacokinetics study was performed in 6 male SD rats (ORIENTBIO Inc., 9 weeks old). Ab417 was purified from the

culture supernatant of the recombinant CHO-DG44 cell line (#9-20) as described above. Ab417 at a dose of 3 or 10 mg/kg was i.v. injected into 3 rats. After indicated time points, blood was collected from the rats and serum was recovered. To determine the serum concentration of Ab417, the sera were subjected to indirect ELISA using hL1-ECD-S1 as a coating antigen. Serum concentrations were determined from standard curves that were generated from known concentrations of purified Ab417. PK parameters ( $AUC_{last}$ ,  $C_{max}$ ,  $T_{max}$ ,  $t_{1/2}$ ,  $CL_T$ ,  $V_d$ , and MRT) were calculated using Phoenix WinNonlin (ver. 6.2, Phasight-A Vertara Company, USA).

### **In vivo antitumor activity of Ab417**

Nude mice (BALB/c Slc-*nu*, 5 weeks old) were obtained from Japan SLC, Inc. (Japan). Choi-Ck cells ( $1 \times 10^6$ ) were inoculated subcutaneously into the right flank of each mouse. Constructed Choi-CK tumor tissue ( $3 \times 3 \times 3 \text{ mm}^3$ ) was inoculated subcutaneously into the back of mice. When tumor volume reached to  $100 \text{ mm}^3$  ( $n = 10$  per group), antibody at a dose of 10 mg/kg was i.v. injected three times per week for 3 weeks. Ab417 and cA10-A3 were produced from the recombinant CHO-DG44 cell lines secreting either antibody.

Tumor growth was monitored by measuring the length and width of the tumor with a caliper and calculating tumor volume on the basis of the following formula;  $TV (\text{mm}^3) = L (\text{mm}) \times W^2 (\text{mm}^2) \times 1/2$ , where L is length and W is width. Body weight of the animals was measured twice a week. At the end of the experiments, mice were euthanized. Tumor tissues were taken out and weighed. Tumor growth inhibition rate (IR) was calculated as following formula;  $IR (\%) = (1 - T/C) \times 100$ , where T is mean tumor weight of the test substance group and C is mean tumor weight of the negative control group.

### **Statistical analysis**

Data are presented as mean  $\pm$  SD and statistical comparisons between groups were performed using one-way analysis of variance (ANOVA) followed by Dunnett's t-test or Steel's test. A value of  $p < 0.05$  was considered significant.

### **Disclosure of potential conflicts of interest**

No potential conflicts of interest were disclosed.

### **Acknowledgments**

This research was supported by a grant (C1007150-01-01) from the Ministry of Science and Technology of Korea and a grant (KDDF-201212-12) from the Korea Drug Development Fund (KDDF) funded by Ministry of Science, ICT and Future Planning, Ministry of Trade, Industry & Energy and Ministry of Health & Welfare, and 2015 Research Grant from Kangwon National University (No. 520150322).

### **References**

- Haspel J, Grumet M. The L1CAM extracellular region: a multi-domain protein with modular and cooperative binding modes. *Front Biosci* 2003; 8:s1210-25; PMID:12957823; <http://dx.doi.org/10.2741/1108>
- Rathjen FG, Schachner M. Immunocytological and biochemical characterization of a new neuronal cell surface component (L1 antigen) which is involved in cell adhesion. *EMBO J* 1984; 3:1-10; PMID:6368220
- Pancook JD, Reisfeld RA, Varki N, Vitiello A, Fox RI, Montgomery AM. Expression and regulation of the neural cell adhesion molecule L1 on human cells of myelomonocytic and lymphoid origin. *J Immunol* 1997; 158:4413-21; PMID:9127006
- Debiec H, Christensen EI, Ronco PM. The cell adhesion molecule L1 is developmentally regulated in the renal epithelium and is involved in kidney branching morphogenesis. *J Cell Biol* 1998; 143:2067-79; PMID:9864376; <http://dx.doi.org/10.1083/jcb.143.7.2067>
- Thor G, Probstmeier R, Schachner M. Characterization of the cell adhesion molecules L1, N-CAM and J1 in the mouse intestine. *EMBO J* 1987; 6:2581-6; PMID:3315649
- Raveh S, Gavert N, Ben-Ze'ev A. L1 cell adhesion molecule (L1CAM) in invasive tumors. *Cancer Lett* 2009; 282:137-45; PMID:19144458; <http://dx.doi.org/10.1016/j.canlet.2008.12.021>
- Kiefel H, Bondong S, Erbe-Hoffmann N, Hazin J, Riedle S, Wolf J, Pfeifer M, Arlt A, Schäfer H, Mürköster SS, et al. L1CAM-integrin interaction induces constitutive NF-kappaB activation in pancreatic adenocarcinoma cells by enhancing IL-1beta expression. *Oncogene* 2010; 29:4766-78; PMID:20543863; <http://dx.doi.org/10.1038/onc.2010.230>
- Kiefel H, Bondong S, Pfeifer M, Schirmer U, Erbe-Hoffmann N, Schäfer H, Sebens S, Altevogt P. EMT-associated up-regulation of L1CAM provides insights into L1CAM-mediated integrin signalling and NF-kB activation. *Carcinogenesis* 2012; 33:1919-29; PMID:22764136; <http://dx.doi.org/10.1093/carcin/bgs220>
- Hall H, Walsh FS, Doherty P. Review: a role for the FGF receptor in the axonal growth response stimulated by cell adhesion molecules? *Cell Adhes Commun* 1996; 3:441-50; PMID:8807188; <http://dx.doi.org/10.3109/15419069609081021>
- Donier E, Gomez-Sanchez JA, Grijota-Martinez C, Lakoma J, Baars S, Garcia-Alonso L, Cabedo H. L1CAM binds ErbB receptors through Ig-like domains coupling cell adhesion and neuregulin signalling. *PLoS One* 2012; 7:e40674; PMID:22815787; <http://dx.doi.org/10.1371/journal.pone.0040674>
- Gouveia RM, Gomes CM, Sousa M, Alves PM, Costa J. Kinetic analysis of L1 homophilic interaction: role of the first four immunoglobulin domains and implications on binding mechanism. *J Biol Chem* 2008; 283:28038-47; PMID:18701456; <http://dx.doi.org/10.1074/jbc.M804991200>
- Haspel J, Friedlander DR, Ivgy-May N, Chickramane S, Roonprapunt C, Chen S, Schachner M, Grumet M. Critical and optimal Ig domains for promotion of neurite outgrowth by L1/Ng-CAM. *J Neurobiol* 2000; 42:287-302; PMID:10645969; [http://dx.doi.org/10.1002/\(SICI\)1097-4695\(20000215\)42:3%3c287::AID-NEU1%3e3.0.CO;2-X](http://dx.doi.org/10.1002/(SICI)1097-4695(20000215)42:3%3c287::AID-NEU1%3e3.0.CO;2-X)
- Yip PM, Zhao X, Montgomery AM, Siu CH. The Arg-Gly-Asp motif in the cell adhesion molecule L1 promotes neurite outgrowth via interaction with the alphavbeta3 integrin. *Mol Biol Cell* 1998; 9:277-90; PMID:9450954; <http://dx.doi.org/10.1091/mbc.9.2.277>
- Kulahin N, Li S, Hinsby A, Kiselyov V, Berezin V, Bock E. Fibronectin type III (FN3) modules of the neuronal cell adhesion molecule L1 interact directly with the fibroblast growth factor (FGF) receptor. *Mol Cell Neurosci* 2008; 37:528-36; PMID:18222703; <http://dx.doi.org/10.1016/j.mcn.2007.12.001>
- Silletti S, Yebra M, Perez B, Cirulli V, McMahon M, Montgomery AM. Extracellular signal-regulated kinase (ERK)-dependent gene expression contributes to L1 cell adhesion molecule-dependent motility and invasion. *J Biol Chem* 2004; 279:28880-8; PMID:15128735; <http://dx.doi.org/10.1074/jbc.M404075200>
- Gavert N, Conacci-Sorrell M, Gast D, Schneider A, Altevogt P, Brabletz T, Ben-Ze'ev A. L1, a novel target of beta-catenin signaling, transforms cells and is expressed at the invasive front of colon cancers. *J Cell Biol* 2005; 168:633-42; PMID:15716380; <http://dx.doi.org/10.1083/jcb.200408051>
- Zecchini S, Bianchi M, Colombo N, Fasani R, Goisis G, Casadio C, Viale G, Liu J, Herlyn M, Godwin AK, et al. The differential role of L1 in ovarian carcinoma and normal ovarian surface epithelium. *Cancer*

- Res 2008; 68:1110-8; PMID:18281486; <http://dx.doi.org/10.1158/0008-5472.CAN-07-2897>
18. Min JK, Kim JM, Li S, Lee JW, Yoon H, Ryu CJ, Jeon SH, Lee JH, Kim JY, Yoon HK, et al. L1 cell adhesion molecule is a novel therapeutic target in intrahepatic cholangiocarcinoma. *Clin Cancer Res* 2010; 16:3571-80; PMID:20501614; <http://dx.doi.org/10.1158/1078-0432.CCR-09-3075>
  19. Jung J, Son YS, Park H, Jeon SK, Lee JW, Choi SY, Kim JM, Kwon YG, Hong HJ, Min JK. The cell adhesion molecule L1 promotes gallbladder carcinoma progression in vitro and in vivo. *Oncol Rep* 2011; 25:945-52; PMID:21318226; <http://dx.doi.org/10.3892/or.2011.1181>
  20. Sebens Muerkoster S, Werbing V, Sipos B, Debus MA, Witt M, Grossmann M, Leisner D, Kötteritzsch J, Kappes H, Klöppel G, et al. Drug-induced expression of the cellular adhesion molecule L1CAM confers anti-apoptotic protection and chemoresistance in pancreatic ductal adenocarcinoma cells. *Oncogene* 2007; 26:2759-68; PMID:17086212; <http://dx.doi.org/10.1038/sj.onc.1210076>
  21. Ben Q, An W, Fei J, Xu M, Li G, Li Z, Yuan Y. Downregulation of L1CAM inhibits proliferation, invasion and arrests cell cycle progression in pancreatic cancer cells. *Exp Ther Med* 2014; 7:785-90; PMID:24660028
  22. Yoon H, Min JK, Lee DG, Kim DG, Koh SS, Hong HJ. L1 cell adhesion molecule and epidermal growth factor receptor activation confer cisplatin resistance in intrahepatic cholangiocarcinoma cells. *Cancer Lett* 2012; 316:70-6; PMID:22088438; <http://dx.doi.org/10.1016/j.canlet.2011.10.024>
  23. Magrini E, Villa A, Angiolini F, Doni A, Mazzarol G, Rudini N, Madaluno L, Komuta M, Topal B, Prenen H, et al. Endothelial deficiency of L1 reduces tumor angiogenesis and promotes vessel normalization. *J Clin Invest* 2014; 124:4335-50; PMID:25157817; <http://dx.doi.org/10.1172/JCI70683>
  24. Grage-Griebenow E, Jerg E, Gorys A, Wicklein D, Wesch D, Freitag-Wolf S, Goebel L, Vogel I, Becker T, Ebsen M, et al. L1CAM promotes enrichment of immunosuppressive T cells in human pancreatic cancer correlating with malignant progression. *Mol Oncol* 2014; 8:982-97; PMID:24746181; <http://dx.doi.org/10.1016/j.molonc.2014.03.001>
  25. Slamon DJ, Leyland-Jones B, Shak S, Fuchs H, Paton V, Bajamonde A, Fleming T, Eiermann W, Wolter J, Pegram M, et al. Use of chemotherapy plus a monoclonal antibody against HER2 for metastatic breast cancer that overexpresses HER2. *N Engl J Med* 2001; 344:783-92; PMID:11248153; <http://dx.doi.org/10.1056/NEJM200103153441101>
  26. Smith IE. Trastuzumab for early breast cancer. *Lancet* 2006; 367:107; PMID:16413866; [http://dx.doi.org/10.1016/S0140-6736\(06\)67951-8](http://dx.doi.org/10.1016/S0140-6736(06)67951-8)
  27. Baselga J, Swain SM. Novel anticancer targets: revisiting ERBB2 and discovering ERBB3. *Nat Rev Cancer* 2009; 9:463-75; PMID:19536107; <http://dx.doi.org/10.1038/nrc2656>
  28. Cunningham D, Humblet Y, Siena S, Khayat D, Bleiberg H, Santoro A, Bets D, Mueser M, Harstrick A, Verslype C, et al. Cetuximab monotherapy and cetuximab plus irinotecan in irinotecan-refractory metastatic colorectal cancer. *N Engl J Med* 2004; 351:337-45; PMID:15269313; <http://dx.doi.org/10.1056/NEJMoa033025>
  29. Arlt MJ, Novak-Hofer I, Gast D, Gschwend V, Moldenhauer G, Grunberg J, Honer M, Schubiger PA, Altevogt P, Krüger A. Efficient inhibition of intra-peritoneal tumor growth and dissemination of human ovarian carcinoma cells in nude mice by anti-L1-cell adhesion molecule monoclonal antibody treatment. *Cancer Res* 2006; 66:936-43; PMID:16424028; <http://dx.doi.org/10.1158/0008-5472.CAN-05-1818>
  30. Wolterink S, Moldenhauer G, Fogel M, Kiefel H, Pfeifer M, Luttgau S, Gouveia R, Costa J, Endell J, Moebius U, et al. Therapeutic antibodies to human L1CAM: functional characterization and application in a mouse model for ovarian carcinoma. *Cancer Res* 2010; 70:2504-15; PMID:20215505; <http://dx.doi.org/10.1158/0008-5472.CAN-09-3730>
  31. Lee ES, Jeong MS, Singh R, Jung J, Yoon H, Min JK, Kim KH, Hong HJ. A chimeric antibody to L1 cell adhesion molecule shows therapeutic effect in an intrahepatic cholangiocarcinoma model. *Exp Mol Med* 2012; 44:293-302; PMID:22248567; <http://dx.doi.org/10.3858/emmm.2012.44.4.027>
  32. McCafferty J, Griffiths AD, Winter G, Chiswell DJ. Phage antibodies: filamentous phage displaying antibody variable domains. *Nature* 1990; 348:552-4; PMID:2247164; <http://dx.doi.org/10.1038/348552a0>
  33. Winter G, Griffiths AD, Hawkins RE, Hoogenboom HR. Making antibodies by phage display technology. *Annu Rev Immunol* 1994; 12:433-55; PMID:8011287; <http://dx.doi.org/10.1146/annurev.iy.12.040194.002245>
  34. Boder ET, Wittrup KD. Yeast surface display for screening combinatorial polypeptide libraries. *Nat Biotechnol* 1997; 15:553-7; PMID:9181578; <http://dx.doi.org/10.1038/nbt0697-553>
  35. Zhou H, Zhang YL, Lu G, Ji H, Rodi CP. Recombinant antibody libraries and selection technologies. *N Biotechnol* 2011; 28:448-52; PMID:21477669; <http://dx.doi.org/10.1016/j.nbt.2011.03.013>
  36. Bradbury AR, Sidhu S, Dubel S, McCafferty J. Beyond natural antibodies: the power of in vitro display technologies. *Nat Biotechnol* 2011; 29:245-54; PMID:21390033; <http://dx.doi.org/10.1038/nbt.1791>
  37. Chao G, Lau WL, Hackel BJ, Sazinsky SL, Lippow SM, Wittrup KD. Isolating and engineering human antibodies using yeast surface display. *Nat Protoc* 2006; 1:755-68; PMID:17406305; <http://dx.doi.org/10.1038/nprot.2006.94>
  38. Khan SA, Thomas HC, Davidson BR, Taylor-Robinson SD. Cholangiocarcinoma. *Lancet* 2005; 366:1303-14; PMID:16214602; [http://dx.doi.org/10.1016/S0140-6736\(05\)67530-7](http://dx.doi.org/10.1016/S0140-6736(05)67530-7)
  39. Valle J, Wasan H, Palmer DH, Cunningham D, Anthony A, Maraveyas A, Madhusudan S, Iveson T, Hughes S, Pereira SP, et al. Cisplatin plus gemcitabine versus gemcitabine for biliary tract cancer. *N Engl J Med* 2010; 362:1273-81; PMID:20375404; <http://dx.doi.org/10.1056/NEJMoa0908721>
  40. Rizvi S, Borad MJ, Patel T, Gores GJ. Cholangiocarcinoma: molecular pathways and therapeutic opportunities. *Semin Liver Dis* 2014; 34:456-64; PMID:25369307; <http://dx.doi.org/10.1055/s-0034-1394144>
  41. Li S, Jo YS, Lee JH, Min JK, Lee ES, Park T, Kim JM, Hong HJ. L1 cell adhesion molecule is a novel independent poor prognostic factor of extrahepatic cholangiocarcinoma. *Clin Cancer Res* 2009; 15:7345-51; PMID:19920102; <http://dx.doi.org/10.1158/1078-0432.CCR-09-0959>
  42. Choi SY, Jo YS, Huang SM, Liang ZL, Min JK, Hong HJ, Kim JM. L1 cell adhesion molecule as a novel independent poor prognostic factor in gallbladder carcinoma. *Hum Pathol* 2011; 42:1476-83; PMID:21496863; <http://dx.doi.org/10.1016/j.humpath.2011.01.003>
  43. Wei CH, Lee ES, Jeon JY, Heo YS, Kim SJ, Jeon YH, Kim KH, Hong HJ, Ryu SE. Structural mechanism of the antigen recognition by the L1 cell adhesion molecule antibody A10-A3. *FEBS Lett* 2011; 585:153-8; PMID:21094640; <http://dx.doi.org/10.1016/j.febslet.2010.11.028>
  44. Weidle UH, Eggle D, Klostermann S. L1-CAM as a target for treatment of cancer with monoclonal antibodies. *Anticancer Res* 2009; 29:4919-31; PMID:20044598
  45. Mechttersheimer S, Gutwein P, Agmon-Levin N, Stoeck A, Oleszewski M, Riedle S, Postina R, Fahrenholz F, Fogel M, Lemmon V, et al. Ectodomain shedding of L1 adhesion molecule promotes cell migration by autocrine binding to integrins. *J Cell Biol* 2001; 155:661-73; PMID:11706054; <http://dx.doi.org/10.1083/jcb.200101099>
  46. Schafer H, Dieckmann C, Kornienko O, Moldenhauer G, Kiefel H, Salnikov A, Krüger A, Altevogt P, Sebens S. Combined treatment of L1CAM antibodies and cytostatic drugs improve the therapeutic response of pancreatic and ovarian carcinoma. *Cancer Lett* 2012; 319:66-82; PMID:22210381; <http://dx.doi.org/10.1016/j.canlet.2011.12.035>
  47. Kiefel H, Bondong S, Hazin J, Ridinger J, Schirmer U, Riedle S, Altevogt P. L1CAM: a major driver for tumor cell invasion and motility. *Cell Adh Migr* 2012; 6:374-84; PMID:22796939; <http://dx.doi.org/10.4161/cam.20832>
  48. Donato R, Miljan EA, Hines SJ, Aouabdi S, Pollock K, Patel S, Edwards FA, Sinden JD. Differential development of neuronal physiological responsiveness in two human neural stem cell lines. *BMC Neurosci* 2007; 8:36; PMID:17531091; <http://dx.doi.org/10.1186/1471-2202-8-36>
  49. Urlaub G, Kas E, Carothers AM, Chasin LA. Deletion of the diploid dihydrofolate reductase locus from cultured mammalian cells. *Cell* 1983; 33:405-12; PMID:6305508; [http://dx.doi.org/10.1016/0092-8674\(83\)90422-1](http://dx.doi.org/10.1016/0092-8674(83)90422-1)
  50. Jung E, Lee J, Hong HJ, Park I, Lee Y. RNA recognition by a human antibody against brain cytoplasmic 200 RNA. *RNA* 2014; 20:805-14; PMID:24759090; <http://dx.doi.org/10.1261/rna.040899.113>

51. Oh MS, Kim KS, Jang YK, Maeng CY, Min SH, Jang MH, Yoon SO, Kim JH, Hong HJ. A new epitope tag from hepatitis B virus preS1 for immunodetection, localization and affinity purification of recombinant proteins. *J Immunol Methods* 2003; 283:77-89; PMID:14659901; <http://dx.doi.org/10.1016/j.jim.2003.08.010>
52. Coomber DW. Panning of antibody phage-display libraries. Standard protocols. *Methods Mol Biol* 2002; 178:133-45; PMID:11968482
53. Yoon SO, Lee TS, Kim SJ, Jang MH, Kang YJ, Park JH, Kim KS, Lee HS, Ryu CJ, Gonzales NR, et al. Construction, affinity maturation, and biological characterization of an anti-tumor-associated glycoprotein-72 humanized antibody. *J Biol Chem* 2006; 281:6985-92; PMID:16407221; <http://dx.doi.org/10.1074/jbc.M511165200>
54. Lee CV, Liang WC, Dennis MS, Eigenbrot C, Sidhu SS, Fuh G. High-affinity human antibodies from phage-displayed synthetic Fab libraries with a single framework scaffold. *J Mol Biol* 2004; 340:1073-93; PMID:15236968; <http://dx.doi.org/10.1016/j.jmb.2004.05.051>